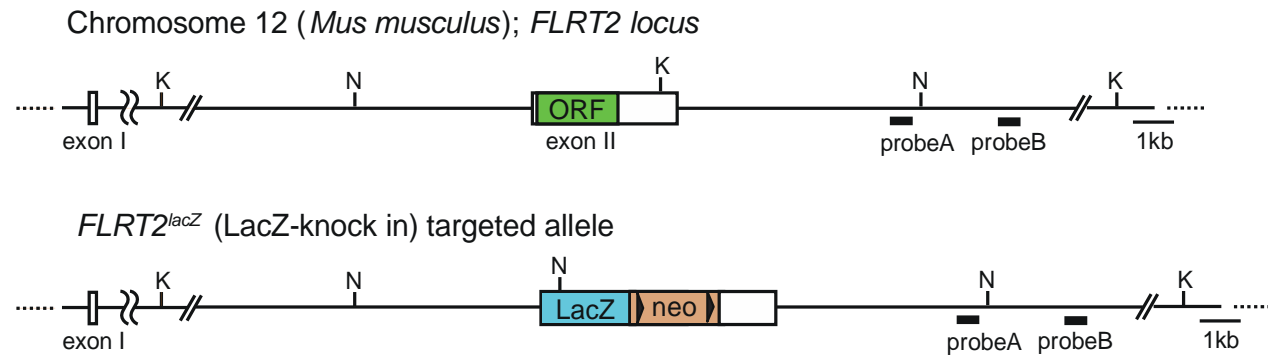


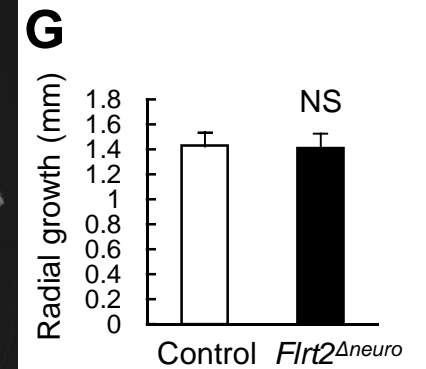
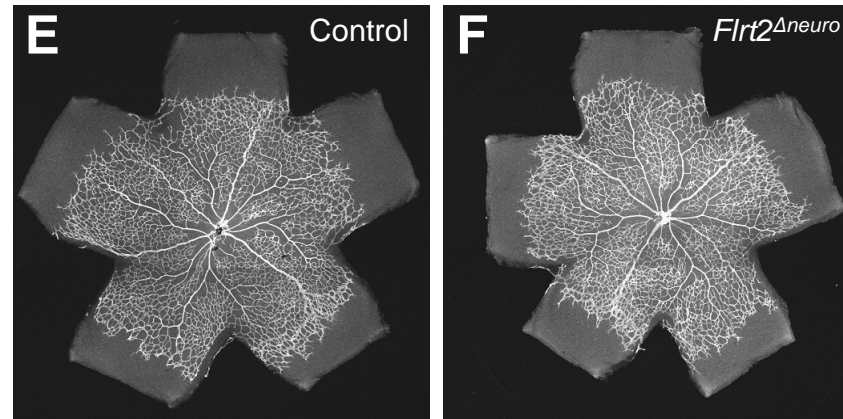
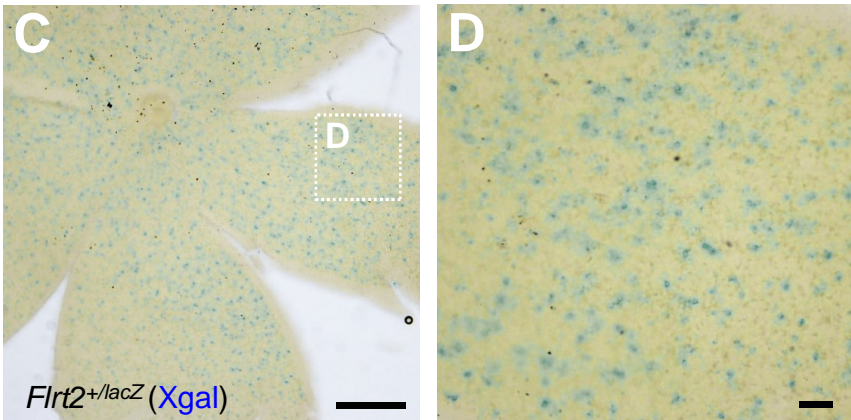
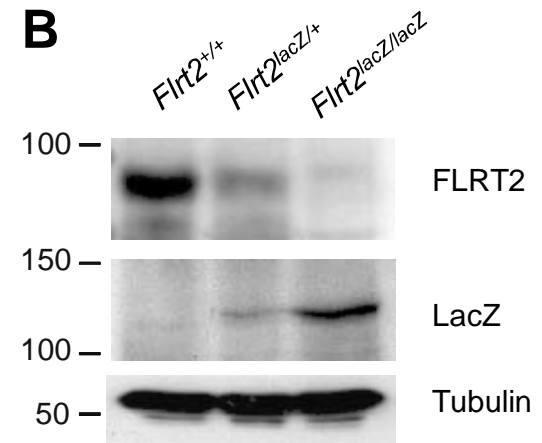
Supplementary Figure 1. Expression patterns of Cre in each Cre line.

(A–F) Expression of green fluorescent protein (GFP) was used as a reporter of *Cre* expression. Whole-mount immunostaining of tissues at embryonic day (E)12.5. (G–K) Bright-field views of embryos and hearts, or whole-mount tissues stained with CD31 at E11.5. (L, M) Heart sections stained with the indicated antibodies at E12.5. GFP was detected in endocardial cells (closed arrowheads) and macrophages (open arrowheads). (N–Q) Whole-mount tissues or heart sections at E12.5 stained with the indicated antibodies. GFP was detected in endocardial (closed arrowheads) and some aortic endothelial cells (open arrowheads) and macrophages (arrows). Scale bars: 500 μm (G–I); 50 μm (A–F, J–Q).

A

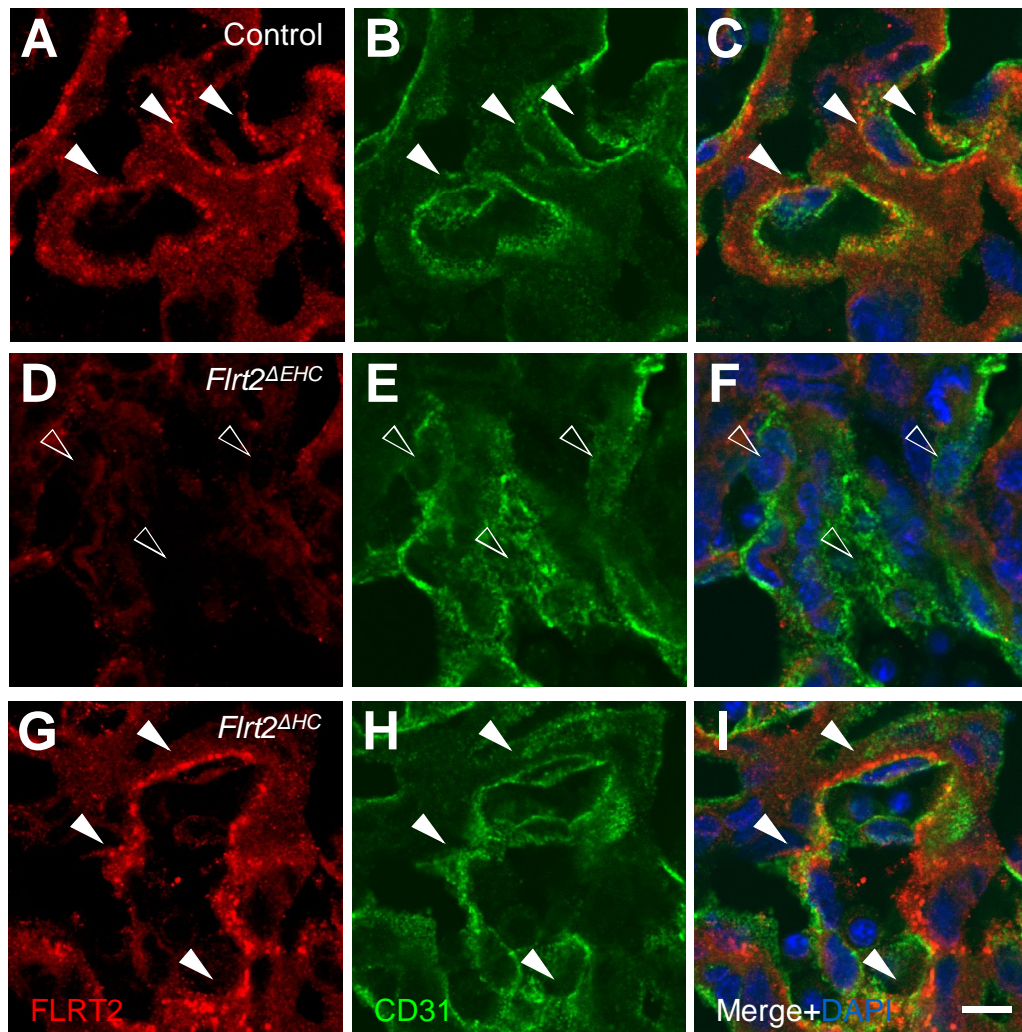


B



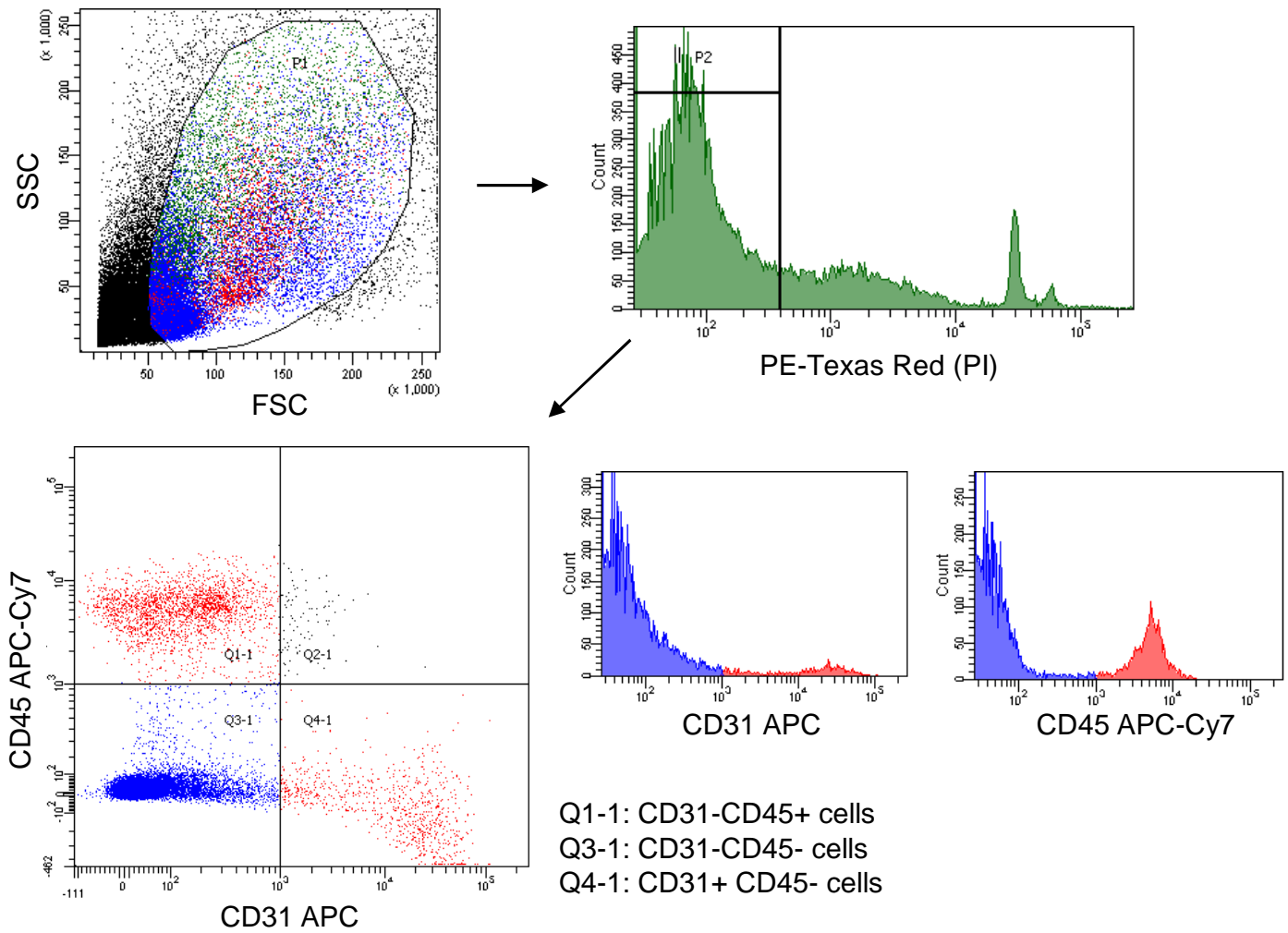
Supplementary Figure 2. *Flrt2* is expressed but is dispensable in postnatal retinal neurons.

(A) Scheme of the *Flrt2*–*LacZ* knock-in allele generated by homologous recombination of exon II, containing the entire open reading frame (ORF) of the mouse *Flrt2* gene. Exon II of the *Flrt2* allele was replaced by a *LacZ* gene followed by a loxP-flanked *PGK*-promoter-driven neomycin gene. Recombination in the embryonic stem cell clone was confirmed by Southern blotting using probes A and B. N, NcoI site for probe A; K, Kpn site for probe B. (B) Western blot analysis showing FLRT2 and β -galactosidase protein levels. Compared with *Flrt2*^{+/+}, FLRT2 protein levels were lower in heterozygotes and absent in *Flrt2*^{lacZ/lacZ} mice, whereas β -galactosidase appeared in heterozygotes and was increased in *Flrt2*^{lacZ/lacZ} mice. Tubulin was used as a loading control. (C, D) X-gal staining of whole-mount retinas at P6. (E–G) Immunohistochemistry and quantification of P6 retinas stained with CD31 ($n = 5$). Scale bars: 500 μ m (C, E, F); 50 μ m (D). NS, not significant. Data are presented as the mean \pm SD.



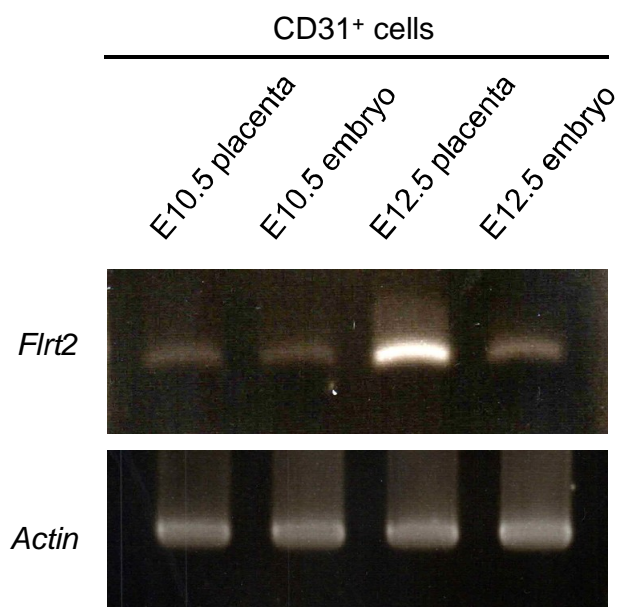
Supplementary Figure 3. FLRT2 protein is detected around placental endothelial cells.

Immunohistochemistry with anti-FLRT2 antibodies on section specimens of placentas at embryonic day (E)12.5. FLRT2 was detected around endothelial cells in control and hematopoietic-specific *Flrt2*-knockout (*Flrt2*^{ΔHC}) mice (closed arrowheads), and this immunoreactivity was diminished in endothelial/hematopoietic-specific *Flrt2*-knockout (*Flrt2*^{ΔEHC}) mice (open arrowheads). Scale bar: 10 μm.



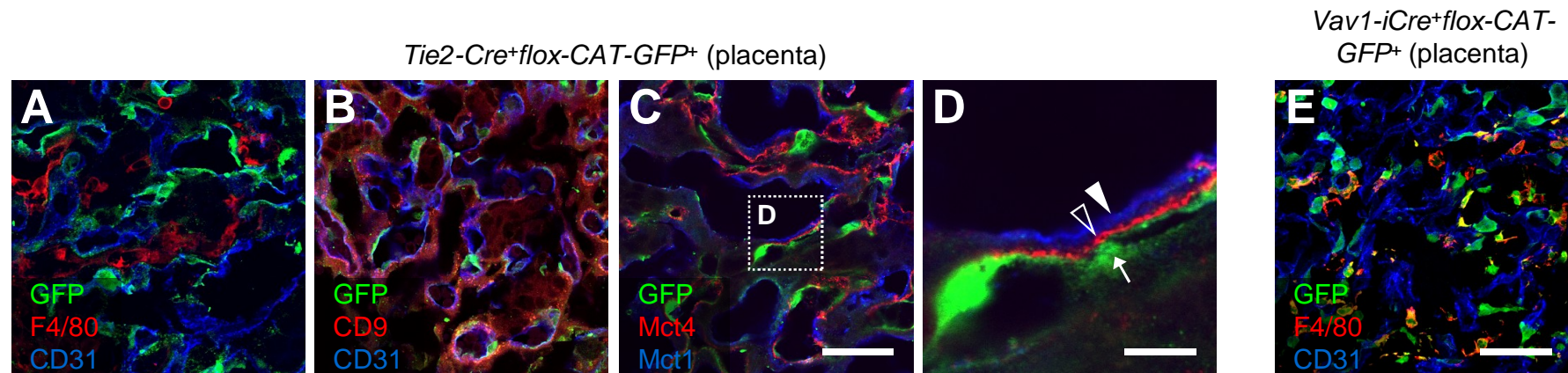
Supplementary Figure 4. Sorting strategy of CD31⁺ or CD45⁺ cells from placental tissues.

Stained samples were sorted by SORP FACS Aria. Debris and dead cells were excluded by forward and side scatter and a negative gate for propidium iodide staining.



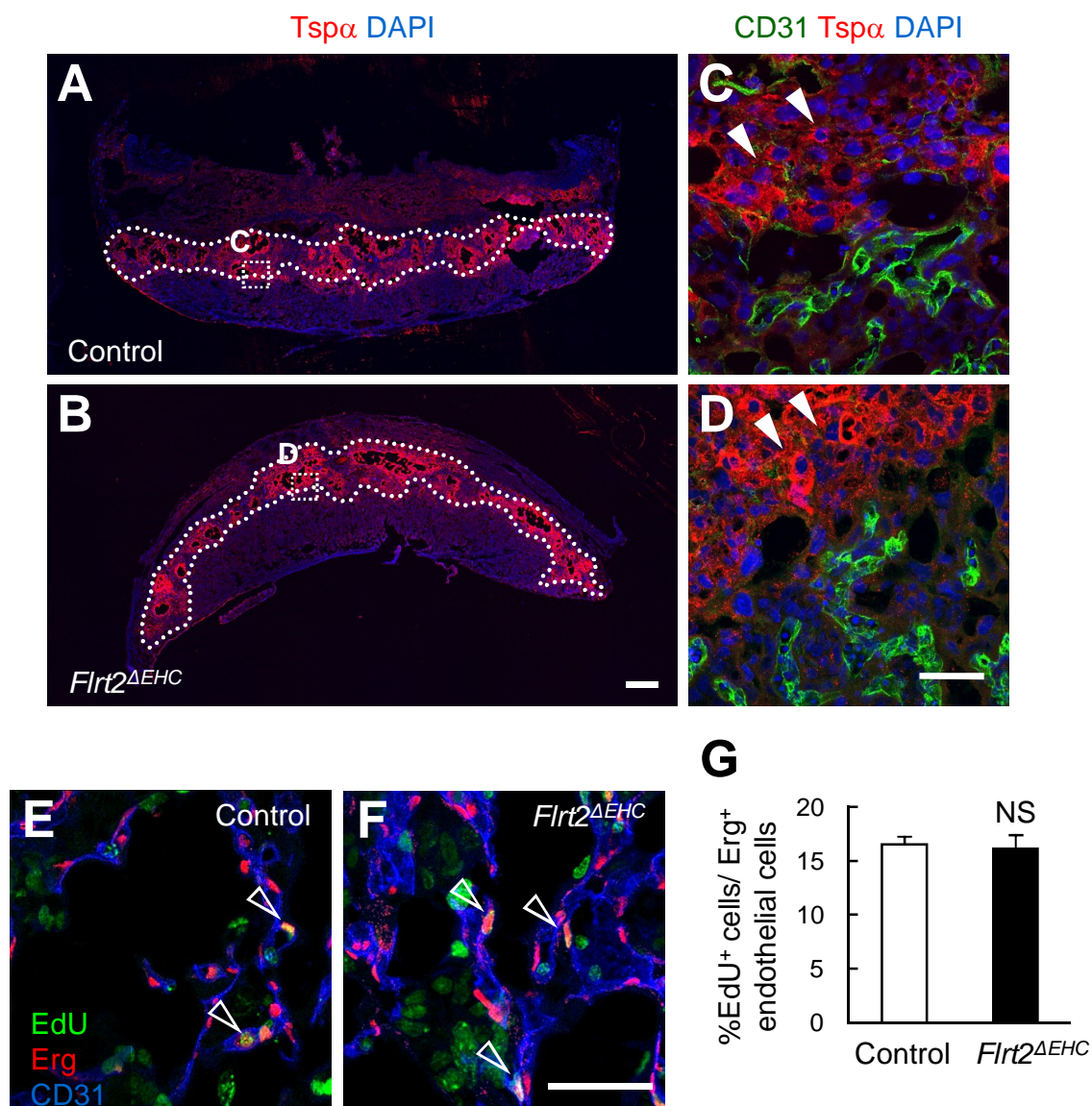
Supplementary Figure 5. *Flrt2* expression in FACS-sorted CD31⁺ endothelial cells.

Flrt2 expression in CD31⁺ endothelial cells, determined by RT-PCR, is abundant in the placenta at embryonic day (E)12.5, compared with placentas and embryos at E10.5.



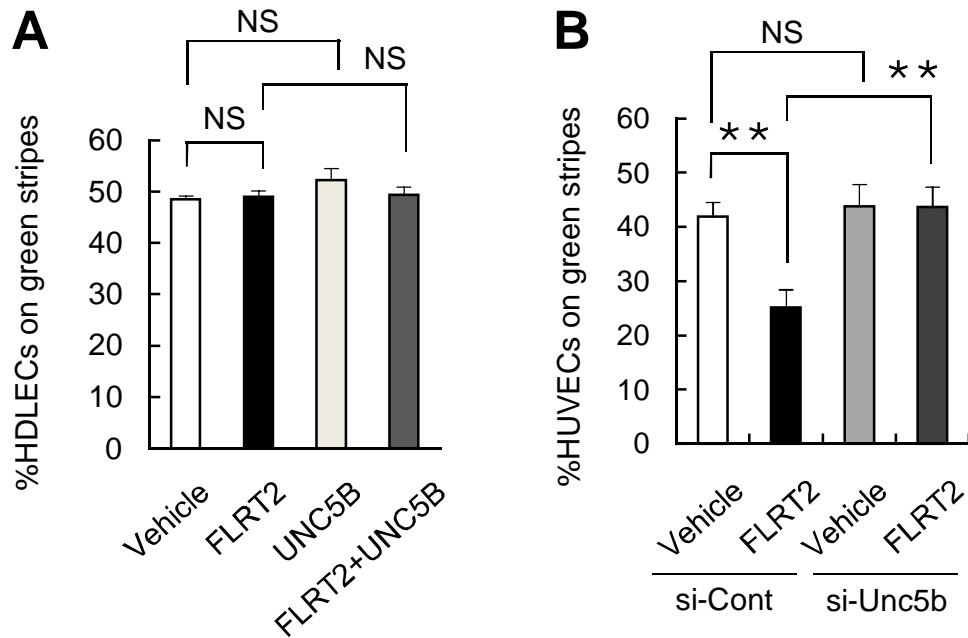
Supplementary Figure 6. Placental expression of *Tie2-Cre/Vav1-iCre*.

Immunohistochemistry of placental sections taken at embryonic day (E)12.5. Cre recombinase expression (indicated by the presence of green fluorescent protein) in placental endothelial cells was detected in *Tie2-Cre* (**A D**) but not in *Vav1-iCre* (**E**) crosses. In *Tie2 Cre* mice, GFP expression was not observed in any trophoblastic-lineage cells marked by CD9, Mct1 (closed arrowhead), or Mct4 (open arrowhead), but was restricted to endothelial cells (arrow) (**D**). Scale bars: 50 μm (**A C, E**); 10 μm (**D**).



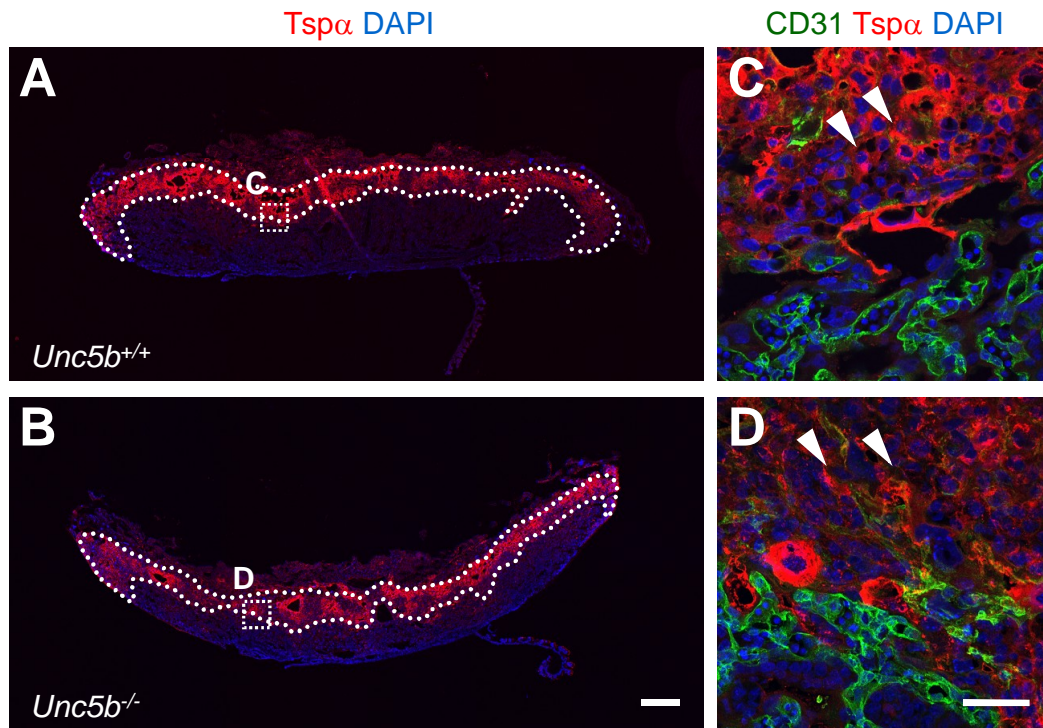
Supplementary Figure 7. Spongiotrophoblasts and endothelial proliferation are not impaired in FLRT2-deficient placentas.

(A–G) Immunohistochemistry and quantification of placental sections taken at embryonic day (E)12.5 ($n = 5$). Areas marked by the dotted line in A, B indicate the spongiotrophoblast layer. The morphology of spongiotrophoblasts (closed arrowheads in C, D) neighboring the labyrinth was not altered in endothelial/hematopoietic-specific *Flrt2*-knockout (*Flrt2* Δ *EHC*) mice. Open arrowheads in E, F indicate proliferating endothelial cells. Scale bars: 500 μ m (A, B); 50 μ m (C–F). NS, not significant. Data are presented as the mean \pm SD.



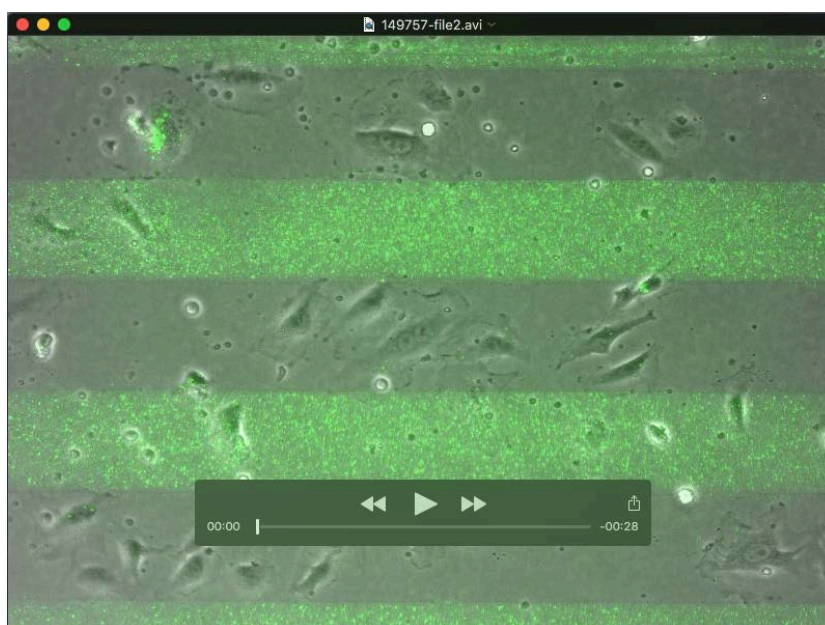
Supplementary Figure 8. FLRT2 repulses endothelial cells through the UNC5B receptor

(A, B) Stripe assays with human dermal lymphatic endothelial cells (HDLECs) or human umbilical vein endothelial cells (HUVECs) under small interfering RNA (siRNA)-mediated knockdown of *Unc5b*, and quantification of the results ($n = 5$). ** $P < 0.01$; NS, not significant. Data are presented as the mean \pm SD.



Supplementary Figure 9. Spongiotrophoblasts are not impaired in *Unc5b*-deficient placentas.

(A–D) Immunohistochemistry of placental sections taken at embryonic day (E)12.5. Areas marked by the dotted line in **A**, **B** indicate the spongiotrophoblast layer. The morphology of spongiotrophoblasts (closed arrowheads in **C**, **D**) neighboring the labyrinth was not altered in *Unc5b*^{-/-} mice. Scale bars: 500 μ m (**A**, **B**); 50 μ m (**C**, **D**).



Supplementary Movie 1. FLRT2 repulses endothelial cells in vitro.

Representative movies of the stripe assay with human umbilical vein endothelial cells (HUVECs) cultured on green stripes coated with FLRT2 proteins.